Observation of chaotic polarization attractors from a graphene mode locked soliton fiber laser

Chang Zhao (赵 畅)[1], Qianqian Huang (黄千千)[1], Mohammed Al Araimi[2], Aleksey Rozhin[3], Sergey Sergeyev[3], and Chengbo Mou (牟成博)[1,*]

[1]*Key Laboratory of Specialty Fiber Optics and Optical Access Networks, Shanghai Institute for Advanced Communication and Data Science, Joint International Research Laboratory of Specialty Fiber Optics and Advanced Communication, Shanghai University, Shanghai 200444, China*

[2]*Higher College of Technology, Al-Khuwair 133, Sultanate of Oman*

[3]*Aston Institute of Photonic Technologies (AIPT), Aston University, Birmingham B4 7ET, UK*

**Corresponding author: mouc1@shu.edu.cn*

Received December 3, 2018; accepted December 27, 2018; posted online January 29, 2019

We have demonstrated an all-fiber passively mode locked erbium-doped fiber laser (EDFL) based on graphene–polyvinyl-alcohol film. By watchfully adjusting the polarization controller, two different polarization attractors, including polarization locked vector solitons and a circular attractor, can be observed. This is first time, to the best of our knowledge, to explore the dynamics polarization attractors exhibited by a vector soliton generated from an EDFL based on graphene.

OCIS codes: 260.5430, 140.3510.

doi: 10.3788/COL201917.020012.

Vector solitons (VSs) have been extensively studied since the propagation of optical pulses in birefringent fibers was theoretically analyzed in 1987[1]. Soon afterwards, VSs were investigated and defined by Christodoulides *et al.* in birefringent nonlinear dispersive media for the first time[2], to the best of our knowledge. A VS is a type of stable-state wave containing two orthogonal polarization components that keep polarization fixed or periodic evolution when propagating in a single mode fiber (SMF) that holds birefringence. Consequently, an SMF can be expected as an ideal vehicle to propagate VSs as a result of the weak birefringence. It is well known that fiber lasers have the ability to generate VSs, utilizing physical saturable absorbers (SAs) such as semiconductor saturable absorption mirrors (SESAMs), carbon nanotube (CNT), and graphene. Besides, in recent years some new two-dimensional (2D) materials, such as black phosphorus[3,4], MXene[5], and bismuthene[6], have been reported to serve as excellent SAs.

Due to the nonlinear coupling between the two orthogonal polarization components, various types of VSs can be formed in the laser cavity. In polarization locked VSs (PLVSs), the state of polarization (SOP) and phase velocity are fixed[7,8], while group velocity locked VSs (GVLVSs) require group velocity locking and no demand for phase velocity locking[9]. Besides, some periodical propagating VSs can be locked to the cavity roundtrip time or its multiples, which are commonly referred as polarization rotation VSs (PRVSs)[10,11]. Some researchers have reported the observation of the vector nature of various dynamic patterns based on figure-eight fiber lasers[12,13]. In the past decade, VSs in passively mode locked fiber lasers using nanomaterial-based SAs have been extensively studied. For instance, polarization dynamics of VSs in the cavity utilizing CNTs have been systematically explored[14–18]. Besides, the iconic 2D material, such as graphene, possesses not only amazing electronic properties but also fantastic optical properties with the potential of operating in a wideband range as a novel SA[19,20]. SAs based on graphene also feature polarization independent saturable absorption[21]. Therefore, for fiber lasers using graphene, intensive investigations have been carried out to study various polarization dynamic patterns and the interaction between two orthogonal polarization components of VSs using a polarization beam splitter (PBS)[19,21–24]. Nevertheless, among all the studies, the phase difference between two orthogonal polarization components and degree of polarization (DOP) are not identified, which can actually be measured with a commercial polarimeter. The missing phase information resulting from the polarization resolved spectral analysis using a PBS may lead to an ambiguous explanation of VSs. Moreover, the tendency of evolution of VSs at a slow time scale from a small number to thousands of roundtrips is defined as asymptotic states (attractors), which could not be resolved by a PBS[15]. A more comprehensive interpretation of the dynamic evolution of VSs is therefore necessary.

In this work, we report the polarization attractors for the first time, to the best of our knowledge, exhibited by VSs operation of an erbium-doped fiber laser (EDFL) based on a graphene–polyvinyl-alcohol (PVA) SA. We have experimentally shown two types of polarization attractors with the single pulse regime. The radio frequency (RF) spectrum indicates ~40 dB signal to noise ratio (SNR) at the fundamental frequency. The demonstrated laser may find applications in secure communication[25], manipulation of atoms and nanoparticles[26–28], and control of magnetization[29].

Figure 1 shows the typical setup of a graphene-based passively mode locked EDFL. The total cavity length is

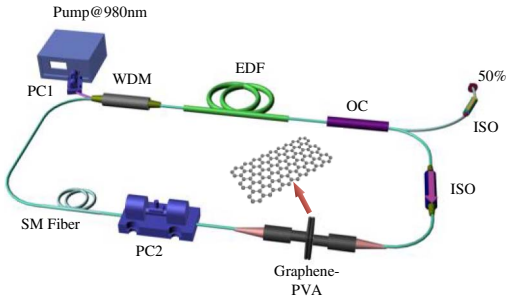

Fig. 1. Schematic setup of the proposed graphene–PVA film mode locked EDFL.

35.7 m, corresponding to the fundamental frequency of 5.84 MHz. An 80 cm highly doped erbium-doped fiber (EDF, OFS EDF80) with a group velocity dispersion of +66.1 ps^2/km makes use of the gain medium in the cavity. In addition, the rest of the fiber is an SMF with an anomalous dispersion of −22 ps^2/km. The total cavity dispersion of the laser is −0.7 ps^2, contributing to the formation of a conventional soliton. A 980 nm laser module (OV LINK) used to produce pump light is injected into the laser cavity through a 980/1550 nm wavelength division multiplexer (WDM). The polarization independent isolator (ISO) in the cavity possesses the ability to guarantee that the pulse transmits in a unidirectional manner. In addition, reflection from the light existing out of the cavity needs to be eliminated by laying an extra ISO outside the cavity. The graphene–PVA film is sandwiched between two fiber connectors to act as a mode locker with the damage threshold of ∼380 mW. An in-line polarization controller (PC2) is used to control the polarization of the cavity or obtain various polarization attractors, and PC1 connected with a pump is involved to optimize cavity anisotropy. Half of the pulse energy is used for intracavity circulation by applying an optical coupler (OC), while the other is implemented for output. Pulse characteristics are detected by an optical spectrum analyzer (OSA, Yokogawa AQ6370C) with a maximum resolution of 0.02 nm, 8 GHz oscilloscope (Keysight DSO90804A), and 3.2 GHz signal analyzer (SSA, 3032X) connected with 12.5 GHz photodetector (Newport 818-BB-51F). The pulse duration of the pulses can be identified by a commercial autocorrelator (Femtochrome, FR-103WS). Furthermore, a commercial polarimeter (Thorlabs, IPM5300) is used with 1 μs resolution, and the distinct attractor can be achieved through 1024 sample points, which are characterized by normalized Stokes parameters s_1, s_2, s_3, and DOP. Output powers of two polarization components, $|u|^2$ and $|\nu|^2$, and phase difference $\Delta\varphi$ are related as follows:

$$
\begin{aligned}
&S_0 = |u|^2 + |\nu|^2, \quad S_1 = |u|^2 - |\nu|^2,\\
&S_2 = 2|u||\nu|\cos\Delta\varphi, \quad S_3 = 2|u||\nu|\sin\Delta\varphi,\\
&s_i = \frac{S_i}{\sqrt{S_1^2 + S_2^2 + S_3^2}}, \quad \mathrm{DOP} = \frac{\sqrt{S_1^2 + S_2^2 + S_3^2}}{S_0}. \qquad (1)
\end{aligned}
$$

For preparation of the graphene SA, ultrasonication of graphite is implemented to get dispersions in deionized (DI) water using a NanoRuptor processor with sodium deoxycholate (SDC). Then, the dispersion is centrifuged (Beckman Coulter Optima Max-XP) followed by mixing with the PVA aqueous solution. The mixing dispersion is then vacuum evaporated at 20°C for a few days, leading to the formation of the composite with 50 μm thickness.

Figure 2(a) shows the nonlinear transmission of graphene film. The modulation depth, saturable intensity, and nonsaturable loss are 5.4%, 0.51 $\mu J/cm^2$, and 78.95%, respectively. Figure 2(b) indicates that the Raman spectroscopic measurement of the produced film is obtained under the excitation of 532 nm. The ubiquitous G peak of graphene in the Raman spectrum caused by the in-plane vibration of sp^2-hybridization carbon with the symmetry of E_{2g} is shown in the picture. The shifts of prominent G and 2D peaks are 1583 and 2688 cm^{-1} respectively, with the intensity ratio (I_{2D}/I_G) of 1.3 corresponding to the formation of few-layer graphene[30]. The D peak generated, owing to the double-resonance process indicating structural disorder, defects as a fingerprint[31]. The stars observed from Fig. 2(b) could be assigned to diffraction peaks associated with the PVA films[32].

The ability of the laser has been measured by an invariance of the pulse and optical spectrum for more than 20 h. We can obtain mode locking under the pump power

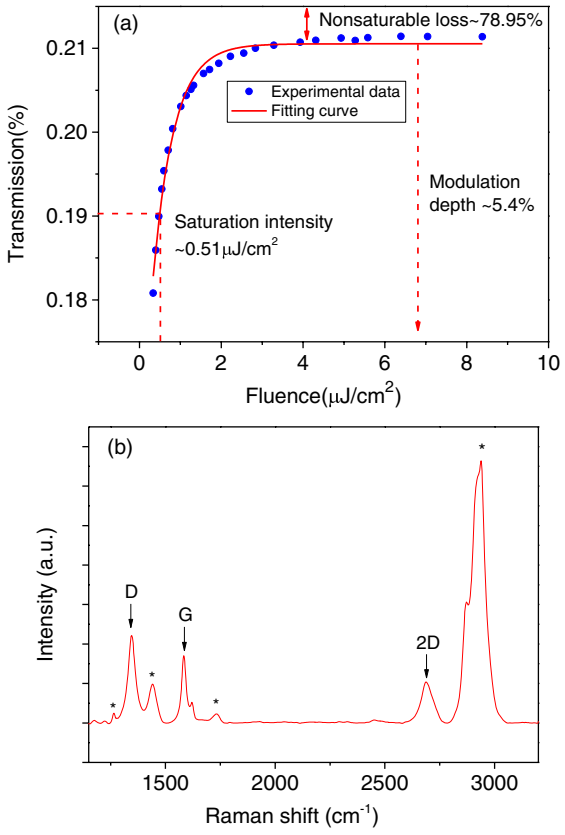

Fig. 2. (a) Nonlinear transmission of graphene SA, (b) Raman spectrum of the graphene SA at 532 nm excitation.

of 9.7 mW. While by increasing pump power, we find that single pulse can be still maintained under the power of 11.6 mW with a strong CW component. PLVSs can be found at the same time. What is more, the maximum pulse energy we can obtain is ~0.1 nJ. The optical spectrum of the PLVS is shown in Fig. 3(a). The pulses center at 1560.6 nm with the 3 dB bandwidth of 1.63 nm. Obviously, the appearance of Kelly sidebands affirms that the laser operates in the conventional soliton regime. The inset in Fig. 3(a) suggests an SNR value of 40 dB. Figure 3(b) is the oscilloscope trace, where the interval between two pulses is 0.171 μs, corresponding to the fundamental frequency of 5.84 MHz. However, the sampling rate of the polarimeter is 1 MHz, which is less than 5.84 MHz, leading to the obtained results being an averaged conclusion. The autocorrelation measurement illustrated in Fig. 3(c) shows that the pulse duration is ~2.4 ps. The output light is divided into two beams through a 50:50 coupler for simultaneous observation of the optical spectrum and SOP. The measured total output power and powers of orthogonal components are shown in Fig. 4(a). Figure 4(b) shows that more than 90% DOP indicates stable output SOP and a fixed phase difference of ~1.2 rad, implying the formation of a PLVS. Such an attractor on the Poincaré sphere in the shape of a focused point is depicted in Fig. 4(c). The complete information of a PLVS is then presented.

We then observe a different attractor during the process of adjusting the PC; the optical spectrum is almost identical. Under the condition, the 3 dB bandwidth of the optical spectrum is 1.98 nm, the period is 0.171 μs, and the pulse duration is 2.5 ps, which is slightly larger than

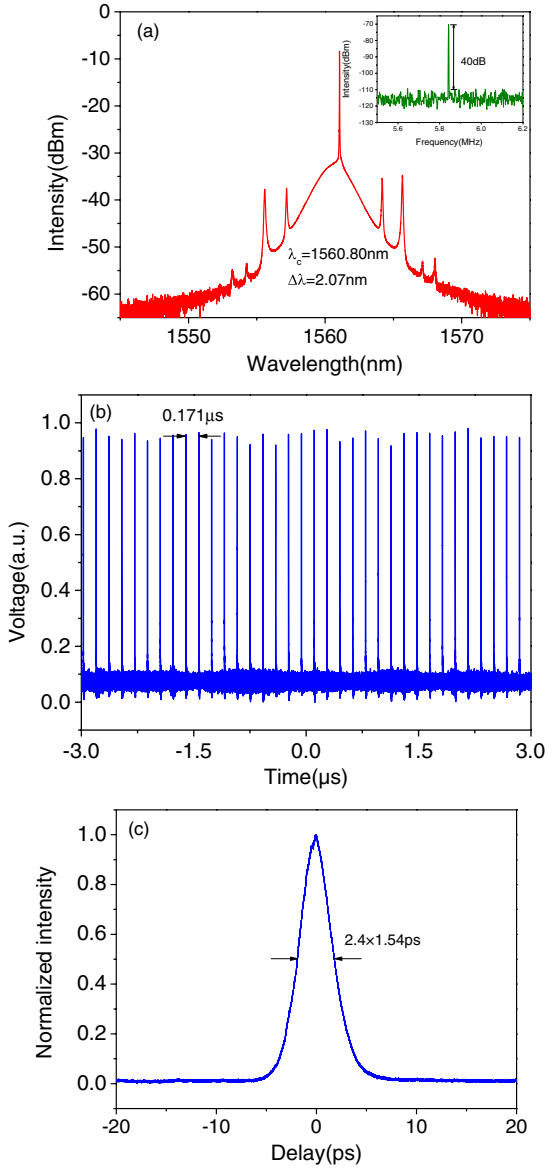

Fig. 3. (a) Optical spectrum, the inset shows the signal noise ratio (SNR) at fundamental frequency, (b) oscilloscope trace, (c) autocorrelation trace.

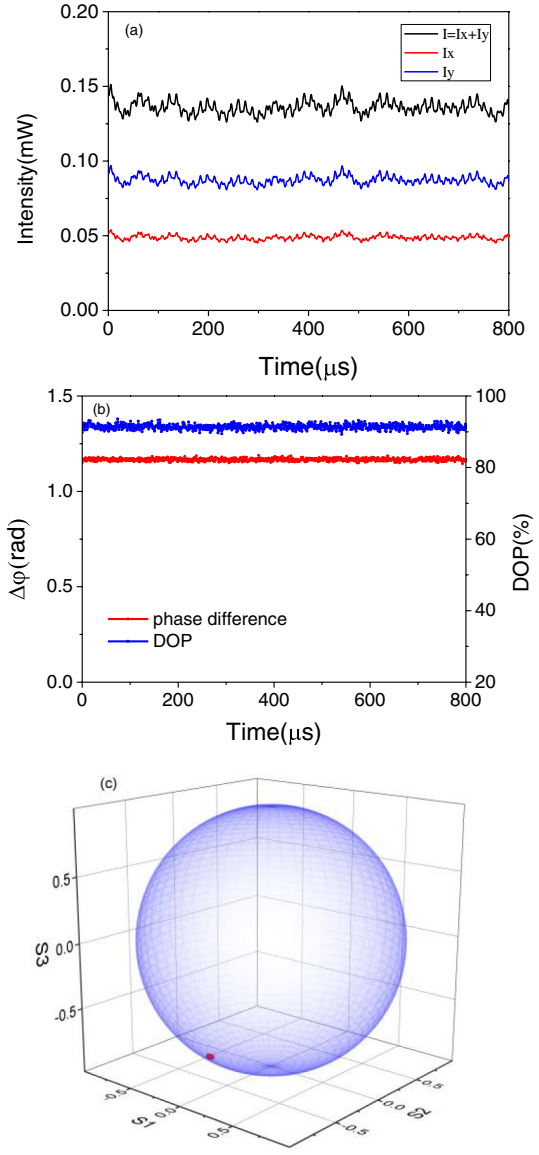

Fig. 4. (a) Optical power of orthogonal component, (b) phase difference and DOP, (c) normalized Stokes parameters shown by Poincaré sphere.

that shown in Fig. 3(c). The inset in Fig. 5(a) demonstrates that the SNR is 39.4 dB, which indicates stability of the attractor [Figs. 5(a)–5(c)]. Optical powers of two orthogonally polarized states and total power are indicated in Fig. 6(a). Obviously, the power of polarization along the y axis is similar to total power, while the polarization along the x axis has a very low power. It is found that DOP of the pulse oscillated around 30% with fast phase difference oscillation, as shown in Fig. 6(b). The resulting trajectory that is winding around a circle on the Poincaré sphere is depicted in Fig. 6(c). We speculate that the low DOP is a result of the fast changing of the SOP. This claims the chaotic polarization attractor on the polarization domain represented by the Poincaré sphere.

The formation of different attractors can be attributed to the existence of coherent coupling between two

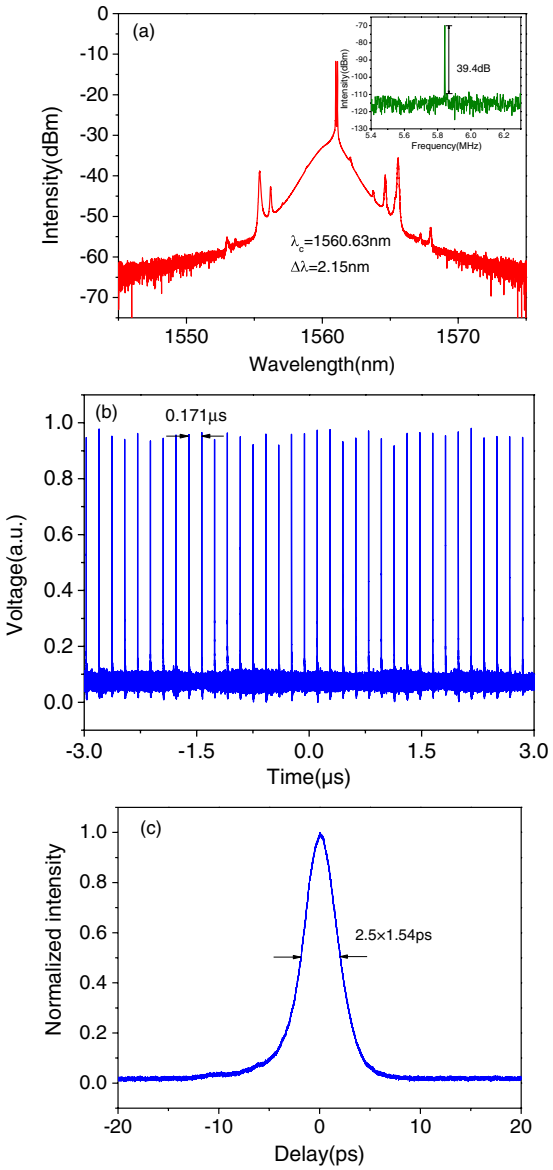

Fig. 5. (a) Optical spectrum, the inset map shows the SNR at fundamental frequency, (b) oscilloscope trace, (c) autocorrelation trace.

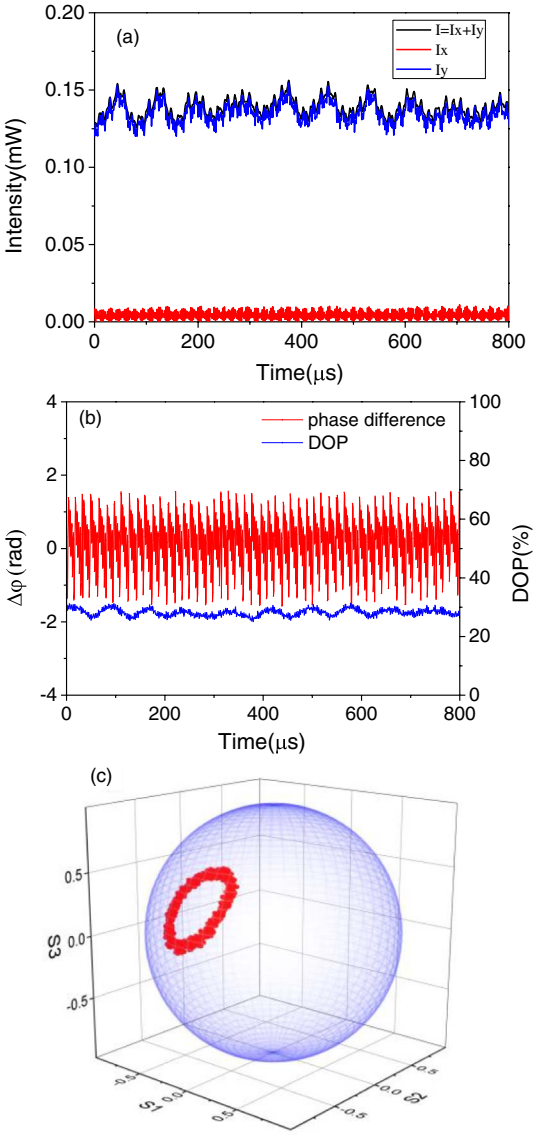

Fig. 6. (a) Optical power of orthogonal component, (b) phase difference and DOP, (c) normalized Stokes parameters shown by Poincaré sphere.

orthogonal polarization components. Pump power, amplitude, and anisotropy of the cavity determine the degree of coupling that controls the formation of polarization attractors. Hence, the polarization attractors shown in Figs. 4 and 6 are caused by increased amplitude and phase anisotropy in the cavity. However, other complex behavior that is not observed in our present work can be the consequence of weaker coupling caused by an isotropic cavity[14]. It is worthy to mention that, during our experiment, there is no Q-switching observed, indicating a high quality graphene SA.

In conclusion, we firstly studied a polarization attractor formed by VS operation of an EDFL based on a graphene–PVA film. Under the power of 11.6 mW, two types of polarization attractors can be obtained by carefully adjusting PCs. One attractor is a PLVS corresponding to a fixed point on the Poincaré sphere with a high DOP of >90%, and the other attractor is an elliptical

trajectory on the Poincaré sphere exhibiting the jump of phase difference between two orthogonal polarization states. The demonstrated work may help in understanding nonlinear optical dynamics in nanomaterial-based ultrafast lasers. It may also provide a neat platform for studying nonlinear optical properties of 2D materials.

The authors acknowledge the National Natural Science Foundation of China (NSFC) (No. 61605107), the Young Eastern Scholar Program at Shanghai Institutions of Higher Learning (No. QD2015027), the Young 1000 Talent Plan Program of China, Open Program of the State Key Laboratory of Advanced Optical Communication Systems and Networks at Shanghai Jiao Tong University, China (No. 2017GZKF17), and the Open Fund of IPOC2017B010 (BUPT) and RAEng/ Leverhulme Trust Senior Research Fellowships (LTSRF1617/13/57).

References

1. C. R. Menyuk, Opt. Lett. **12**, 614 (1987).
2. D. N. Christodoulides and R. I. Joseph, Opt. Lett. **13**, 53 (1988).
3. Z. C. Luo, M. Liu, Z. N. Guo, X. F. Jiang, A. P. Luo, C. J. Zhao, X. F. Yu, W. C. Xu, and H. Zhang, Opt. Express **23**, 20030 (2015).
4. G. Hu, T. Albrow-Owen, X. Jin, A. Ali, Y. Hu, R. C. T. Howe, K. Shehzad, Z. Yang, X. Zhu, R. I. Woodward, T. C. Wu, H. Jussila, J. B. Wu, P. Peng, P. H. Tan, Z. Sun, E. J. R. Kelleher, M. Zhang, Y. Xu, and T. Hasan, Nat. Commun. **8**, 278 (2017).
5. X. Jiang, S. Liu, W. Liang, S. Luo, Z. He, Y. Ge, H. Wang, R. Cao, F. Zhang, and Q. Wen, Laser Photon. Rev. **12**, 1700229 (2017).
6. L. Lu, Z. Liang, L. Wu, Y. X. Chen, Y. Song, S. C. Dhanabalan, J. S. Ponraj, B. Dong, Y. Xiang, and F. Xing, Laser Photon. Rev. **12**, 1700221 (2018).
7. S. T. Cundiff, B. C. Collings, N. N. Akhmediev, J. M. Soto-Crespo, K. Bergman, and W. H. Knox, Phys. Rev. Lett. **82**, 3988 (1999).
8. B. C. Collings, S. T. Cundiff, N. N. Akhmediev, J. M. Sotocrespo, K. Bergman, and W. H. Knox, J. Opt. Soc. Am. B **17**, 354 (2000).
9. D. Y. Tang, H. Zhang, L. M. Zhao, N. Xiang, and X. Wu, Opt. Express **16**, 9528 (2008).
10. L. M. Zhao, D. Y. Tang, H. Zhang, and X. Wu, Opt. Express **16**, 10053 (2008).
11. J. H. Wong, K. Wu, H. H. Liu, C. Ouyang, H. Wang, S. Aditya, P. Shum, S. Fu, E. J. R. Kelleher, A. Chernov, and E. D. Obraztsova, Opt. Commun. **284**, 2007 (2011).
12. L. Yun, X. Liu, and D. Mao, Opt. Express **20**, 20992 (2012).
13. Q. Y. Ning, H. Liu, X. W. Zheng, W. Yu, A. P. Luo, X. G. Huang, Z. C. Luo, W. C. Xu, S. H. Xu, and Z. M. Yang, Opt. Express **22**, 11900 (2014).
14. S. V. Sergeyev, C. Mou, A. Rozhin, and S. K. Turitsyn, Opt. Express **20**, 27434 (2012).
15. C. Mou, S. V. Sergeyev, A. G. Rozhin, and S. K. Turitsyn, Opt. Express **21**, 26868 (2013).
16. V. Tsatourian, S. V. Sergeyev, C. Mou, A. Rozhin, V. Mikhailov, B. Rabin, P. S. Westbrook, and S. K. Turitsyn, Sci. Rep. **3**, 3154 (2013).
17. T. Habruseva, C. Mou, A. Rozhin, and S. V. Sergeyev, Opt. Express **22**, 15211 (2014).
18. S. V. Sergeyev, C. Mou, E. G. Turitsyna, A. Rozhin, S. K. Turitsyn, and K. Blow, Light Sci. Appl. **3**, e131 (2014).
19. H. Zhang, D. Tang, L. Zhao, Q. Bao, and K. P. Loh, Opt. Commun. **283**, 3334 (2010).
20. D. Y. Tang, G. Q. Xie, H. H. Yu, H. J. Zhang, J. Ma, J. Y. Wang, L. J. Qian, P. Lv, P. Yuan, and W. L. Gao, Opt. Lett. **37**, 3165 (2012).
21. Y. F. Song, L. Li, H. Zhang, D. Y. Shen, D. Y. Tang, and K. P. Loh, Opt. Express **21**, 10010 (2013).
22. Y. F. Song, H. Zhang, D. Y. Tang, and D. Y. Shen, Opt. Express **20**, 27283 (2012).
23. Y. F. Song, L. Li, D. Y. Tang, and D. Y. Shen, Laser Phys. Lett. **10**, 125103 (2013).
24. M. Han, S. Zhang, X. Li, H. Zhang, H. Yang, and T. Yuan, Opt. Express **23**, 2424 (2015).
25. G. D. VanWiggeren and R. Roy, Phys. Rev. Lett. **88**, 097903 (2002).
26. M. Spanner, K. M. Davitt, and M. Y. Ivanov, J. Chem. Phys. **115**, 8403 (2001).
27. Y. Jiang, T. Narushima, and H. Okamoto, Nat. Phys. **6**, 1005 (2010).
28. L. Tong, V. D. Miljkovic, and M. Kall, Nano Lett. **10**, 268 (2010).
29. N. Kanda, T. Higuchi, H. Shimizu, K. Konishi, K. Yoshioka, and M. Kuwata-Gonokami, Nat. Commun. **2**, 362 (2011).
30. H. Zhou, F. Yu, H. Yang, C. Qiu, M. Chen, L. Hu, Y. Guo, H. Yang, C. Gu, and L. Sun, Chem. Commun. (Camb) **47**, 9408 (2011).
31. L. M. Malard, M. A. Pimenta, G. Dresselhaus, and M. S. Dresselhaus, Phys. Rep. **473**, 51 (2009).
32. H. R. Chen, C. Y. Tsai, C. Y. Chang, K. H. Lin, C. S. Chang, and W. F. Hsieh, J. Lightwave Technol. **33**, 4406 (2015).